Environmental and Sustainability Indicators 31 (2026) 101316

Contents lists available at ScienceDirect

Environmental and Sustainability Indicators

journal homepage: www.sciencedirect.com/journal/environmental-and-sustainability-indicators

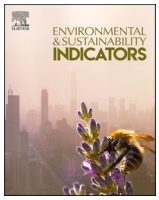

Integrating economic and hydrological scales to develop model-based indicators of water scarcity in local economies

Gino Sturla [a,b], Benedetto Rocchi [c,*], Enrica Caporali [d], Tommaso Pacetti [e]

[a] College UC, Pontificia Universidad Católica de Chile, Chile
[b] Department of Hydraulic and Environmental Engineering, School of Engineering, Pontificia Universidad Católica de Chile, Chile
[c] Department of Economics and Management, University of Florence, Italy
[d] Dipartimento di Ingegneria Civile e Ambientale, Italy
[e] Water Resources Research and Documentation Center, University for Foreigners of Perugia, Italy

ARTICLE INFO

Keywords:
Input-output analysis
Hydrological models
Water scarcity indicators
Green water scartcity
Local economies
Arno river
Tuscany

ABSTRACT

Traditional models that link economic activity and water resources often rely on economic spatial units, overlooking the hydrological significance of river basins—the fundamental units for water-related assessments. This study analyzes water scarcity of local economies through an integrated hydro-economic approach that harmonizes economic and hydrological scales. Specifically, the analysis focuses on five Local Labor Systems located in the upper Arno River basin, Tuscany, Italy. Spatial harmonization is achieved by aligning sub-basins with their corresponding LLS. Water supply is modeled using the Soil and Water Assessment Tool, while blue, green, and grey water demand is estimated through an environmentally extended MultiRegional Input–Output model. These models interact through two key endogenous effects: (i) adjustments in agricultural blue water withdrawals based on green water availability, and (ii) changes in grey water requirements due to variations in water supply. The model characterizes green water availability, allowing for a more realistic representation of agricultural water demand dynamics compared to models that lack physical hydrological integration. Based on different approaches to water supply and demand, five water scarcity indicators are developed for each LLS, two of which are proposed in this study. Notably, a green water scarcity index is introduced—a metric often omitted in water stress assessments. The results reveal the high hydrological and economic heterogeneity within the study area, providing a solid foundation for characterizing multidimensional water scarcity. Moreover, the adopted approach highlights the value of integrating biophysical and economic models within a spatially coherent framework to inform local policies.

1. Introduction

Water scarcity has been characterized at different territorial scales (Alcamo et al., 2000; Hoekstra, 2016). From an economic perspective, national, regional, or local scales are typically used. In contrast, hydrology relies on more appropriate units of analysis such as river basins or sub-basins Chow et al. (1988); Dingman (2015). Although river basins are best suited to characterize hydrological processes, the disaggregation of productive activities generally does not align with these hydrological units (Ridoutt et al., 2018; Wichelns, 2017).

This mismatch between scales and units of analysis is particularly relevant in the assessment of interconnected economic systems. Unlike hydro-economic studies focused on individual rivers basins, such assessments incorporate data from the productive system across an entire region, country, or even globally, disaggregated into local economies or regions (Duarte et al., 2016; Arto et al., 2016; Lenzen et al., 2013; Feng et al., 2014; Sturla et al., 2023). Determining economic variables for each river basin within a region, and subsequently quantifying interregional flows of goods and services, would be highly complex. Moreover, countries do not disaggregate their national accounts based on hydrological boundaries.

Therefore, the most feasible and effective approach is to adjust the hydrological scale to match the economic scale. This allows for the representation of variables such as surface and groundwater supply in a manner that is consistent with economic data.

In this context, the present study focuses on the Tuscany region

* Corresponding author.
E-mail addresses: gssturla@uc.cl (G. Sturla), benedetto.rocchi@unifi.it (B. Rocchi), enrica.caporali@unifi.it (E. Caporali), tommaso.pacetti@unistrapg.it (T. Pacetti).

https://doi.org/10.1016/j.indic.2026.101316
Received 5 January 2026; Received in revised form 6 May 2026; Accepted 10 May 2026
Available online 12 May 2026

(Italy), which constitutes an interesting case study due to the heterogeneity in water resource availability despite its size, the presence of diverse productive sectors, and the concentration of water demand in the Arno River basin, where 70% of the regional GDP is generated (Venturi et al., 2024; Rocchi et al., 2024).

At the regional level, Tuscany does not exhibit significant water scarcity under average conditions (Rocchi et al., 2024). When exposed to hydrological variability, some issues arise—though not severe—particularly concerning surface water resources (Sturla and Rocchi, 2024). However, due to spatial heterogeneity in both climate and productive structure, local water scarcity problems are significant (Pfister et al., 2009; Feng et al., 2014).

The issue of territorial scale in Tuscany's water scarcity was addressed by Rocchi et al. (2026). However, the study faced certain limitations, including the intrinsic characteristics of the model that relies solely on precipitation as a proxy and do not represent physical hydrological processes, and the fact that the hydrological unit of analysis did not correspond to a river basin or sub-basin. Furthermore, since the model did not adopt a physically based approach, it failed to characterize green water availability (soil moisture), which precludes an assessment of green water scarcity—an essential component for accurately simulating the dynamics of agricultural water use.

In order to address these limitations, this study employs a more realistic framework that integrates the physically based hydrological model SWAT (Soil and Water Assessment Tool; Arnold et al., 1998) with an environmentally extended Multi-Regional Input–Output (MRIO) model. The study focuses on five LLSs located in the upper Arno River basin. Hydrological analysis is conducted at the river sub-basin level and aggregated to the LLS scale, thereby aligning the hydrological and economic scales.

The proposed model is integrated with hydrological and economic calculations performed jointly rather than independently. Hydrological components influence the determination of water use intensity coefficients in agriculture, and both economic and hydrological calculations are used to determine grey water through a mixing model. The analysis incorporates climatic variability (2014–2020) and evaluates its impact on the 2017 productive system.

The methodological innovations of this study in the literature are: (i) the alignment of the hydrological system with the economic system within an integrated model at the local scale; (ii) the development of a green water scarcity indicator based on the physically-based characterization of soil moisture availability; (iii) the adequate and physically grounded representation of the substitution dynamics between green and blue water in the agricultural sector; (iv) the estimation of grey water based on a mixing model fed by actual surface runoff and groundwater recharge, and (v) the proposal of a set of indicators that enables a comprehensive representation of integrated blue, grey, and green water scarcity.

The calculations enable the estimation and comparison of five scarcity indicators across the five LLSs analyzed.

This set of water scarcity indicators—including blue, grey, and green water for each LLS—and the various approaches to water supply and demand allow for a detailed, integrated, and multidimensional analysis of water scarcity.

The following section presents the methodology, detailing the components of the hydro-economic model and their interactions, as well as the data used. The subsequent section presents the results, which are then analyzed in the discussion. Finally, the conclusion highlights the key findings of this study.

2. Methods and data

2.1. Methodology overview

The schematic of the methodology used in this study is shown in Fig. 1. The SWAT hydrological model is used to generate the natural supply of blue water (surface and groundwater) and green water (soil moisture) in each LLS. In parallel, the MRIO model allows for the estimation of extended water demand in each LLS, based on water use intensity coefficients and the MRIO table for Tuscany. The hydrological and economic components are linked through: (i) the mixing model used to determine grey water intensity coefficients, which requires information on water supply and demand, as well as water quality parameters; and (ii) the agricultural water use coefficients, which depend on hydrological variability, as this determines the substitution of green water with blue water.

This integration is implemented as a partially coupled (weak coupling) framework with endogenous feedbacks, in which hydrological variables—such as soil moisture, surface runoff, and groundwater recharge—directly influence water demand. Two key mechanisms drive this interaction. First, in the agricultural sector, reductions in soil moisture generate a state-dependent substitution from green to blue water, leading to additional withdrawals from surface and groundwater sources. This process introduces non-proportional responses in water demand, as irrigation requirements emerge only under deficit conditions. Second, grey water requirements depend on hydrological conditions through the mixing model, where runoff and groundwater recharge determine pollutant dilution capacity. Although this relationship is implemented through a linearized formulation, it captures the underlying dependence of water quality constraints on water

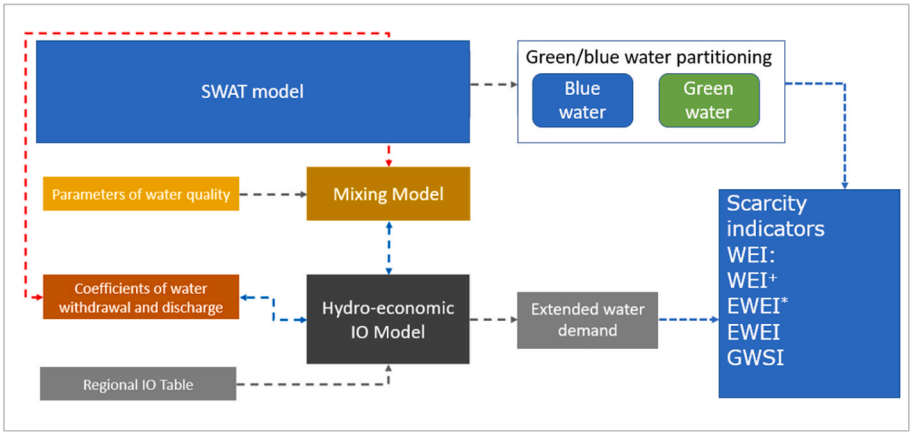

Source: Own elaboration

Fig. 1. Schematic representation of the methodology.
Source: Own elaboration

availability, whereby lower flows increase dilution requirements.

The model operates at an annual scale, with interannual variability driven by the hydrological component. Although the framework does not follow a fully iterative closed-loop structure, this modeling choice allows capturing the dynamic and state-dependent response of water use to hydrological variability while maintaining analytical tractability.

Based on the extended demand and the natural supply, the various scarcity indicators used to characterize water scarcity in the analyzed local economies can be constructed.

2.2. Study area

The study area is the Upper Arno River basin, situated in the Tuscany region of Central Italy, upstream of the La Penna dam. The river basin exhibits diverse topographic and land use characteristics, ranging from mountainous areas to flat agricultural plains. It is part of a broader hydrological system that plays a vital role in regional water resource availability, land productivity, and ecological integrity.

The region experiences a Mediterranean climate, with annual precipitation ranging from 800 to 1800 mm, and a marked seasonality featuring dry summers and wet autumn-winter periods. Soils within the river basin are highly variable—ranging from clay loams to calcareous and silty profiles—which, in combination with land cover patterns, significantly influences runoff, infiltration, and evapotranspiration dynamics.

Different sectors of the river basin exhibit distinct socio-economic and ecohydrological characteristics. The northern mountainous zones are predominantly forested and less densely populated, with lower water demand and relatively preserved hydrological conditions. The southern plains, by contrast, support intensive agricultural activities—both rainfed and irrigated—enabled by substantial irrigation infrastructure and external water inputs. These areas are associated with higher water abstractions, nutrient runoff, and ecological pressure on both surface and groundwater resources. In between, transitional zones combine urban, industrial, and mixed-use landscapes with moderate hydrological regulation and land conversion.

From a hydroeconomic perspective, the Upper Arno River basin is of strategic relevance. It integrates diverse water uses, land functions, and ecological values within a single catchment, making it an ideal case. The adopted spatial boundary of the system analyzed includes the LLS of Arezzo, Bibbiena, Cortona, Montepulciano, and Sinalunga. Fig. 2 illustrates the geographical location of these LLS.

2.3. Hydrological model

To characterize water availability for local economic systems, this study -uses the SWAT model, a semi-distributed, process-based hydrological model that enables spatially explicit simulation of the hydrological cycle at the sub-basin level. SWAT is applied to estimate key components such as surface runoff, groundwater recharge, and soil moisture, the latter serving as a proxy of green water availability relevant for rainfed agriculture. Simulations are performed at a monthly temporal resolution and subsequently aggregated to an annual scale to ensure consistency with the economic modeling framework.

The model setup incorporated a wide range of input data, including climate time series (precipitation, minimum and maximum temperature, solar radiation, relative humidity, wind speed), topography (based on a digital elevation model), land use and land cover, vegetation characteristics, and soil properties, spatially referenced for each Hydrologic Response Unit which represents a discrete area within the watershed defined by a unique combination of soil type, land use, and slope characteristics. Model calibration and validation were conducted using observed streamflow data from hydrometric stations distributed across the upper Arno River basin, following a multi-site and multi-variable calibration approach. This ensured accurate representation of local runoff generation, infiltration, and recharge dynamics, thus enhancing the reliability of simulated water availability indicators. A synthesis of the calibration metrics is reported in Table 1 while the

Table 1
Calibration and validation statistics ranges.

Parameter	Calibration	Validation
R^2	0.71–0.87	0.51–0.75
NSE	0.69–0.79	0.77–0.89
RSR	0.44–0.56	0.49–0.79
PBIAS	−14.70–17.00	−2.30–0.36

Source: Own elaboration

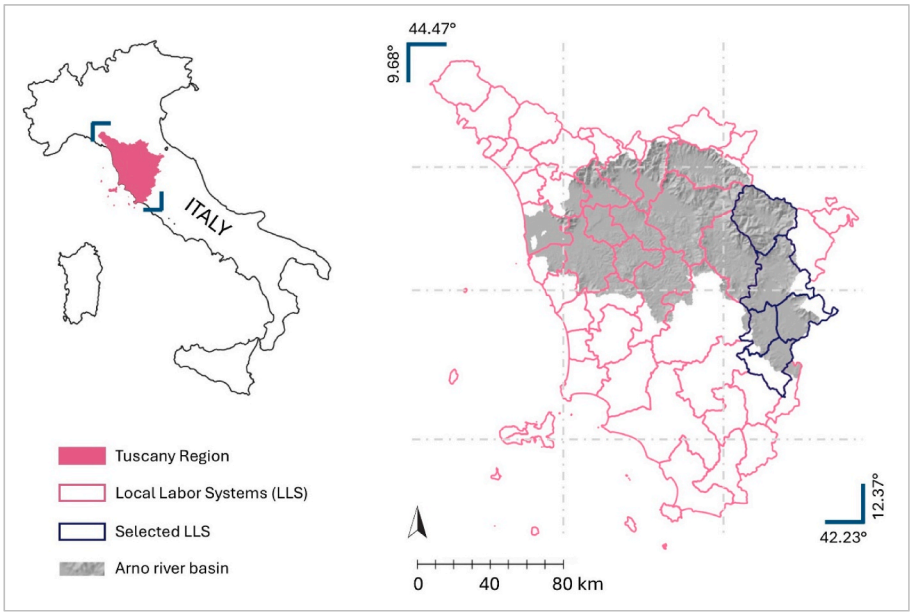

Source: Own elaboration

Fig. 2. Study area: 5 selected LLS with blue boundaries.
Source: Own elaboration

details of the model setup and the calibration can be found in Pacetti et al., (2021).

In addition to the blue water supply generated within the sub-basins, the model also accounts for transfers from the Montedoglio reservoir, located outside the study area (Pacetti et al., 2021).

The hydrological outputs produced at the sub-basin scale are subsequently transferred to the LLS level through a spatial allocation process. Each sub-basin is linked to one or more LLS units based on spatial overlap, determined using GIS-based intersection analysis (Fig. 3). Within each LLS, the hydrological variables—expressed as water depths (e.g., mm)—are weighted according to the proportion of sub-basin area contributing to that LLS. The area-weighted values are then aggregated for each LLS unit. Finally, to obtain volumetric estimates, the aggregated water depths (converted to meters) are multiplied by the surface area (in square meters) of the corresponding LLS unit. This procedure enables the spatial integration of hydrological data across scales, supporting LLS-level water resource assessments.

It is important to note that the spatial boundaries of hydrological units (sub-basins) and economic units (LLS) do not perfectly coincide. To address this mismatch, a spatial intersection approach is applied, whereby each sub-basin is proportionally allocated to one or more LLS units based on the extent of their overlapping areas. Hydrological variables are assumed to be homogeneous within each sub-basin, and their contribution to each LLS is weighted according to the corresponding area shares.

This procedure ensures internal consistency between hydrological and economic scales, while preserving the physical meaning of the simulated variables. Nevertheless, it introduces a degree of spatial aggregation error, particularly in cases where sub-basins exhibit strong internal heterogeneity or when economic activity is unevenly distributed within LLS boundaries. This limitation is inherent to studies that integrate physically based hydrological models with socio-economic units that are not defined by natural boundaries.

Despite this, the adopted approach is consistent with the prevailing practice in integrated hydro-economic modeling, where spatial harmonization is achieved through GIS-based allocation methods. Moreover, the use of relatively small sub-basins and local-scale economic units mitigates potential distortions, ensuring a reasonable level of spatial accuracy for the purposes of this analysis. Importantly, LLS units can be coherently aggregated to sub-basin and river basin levels (Pacetti et al., 2026), which are widely recognized as the appropriate scales for water management and governance (D'Oria et al., 2019; Fatichi and Caporali, 2009).

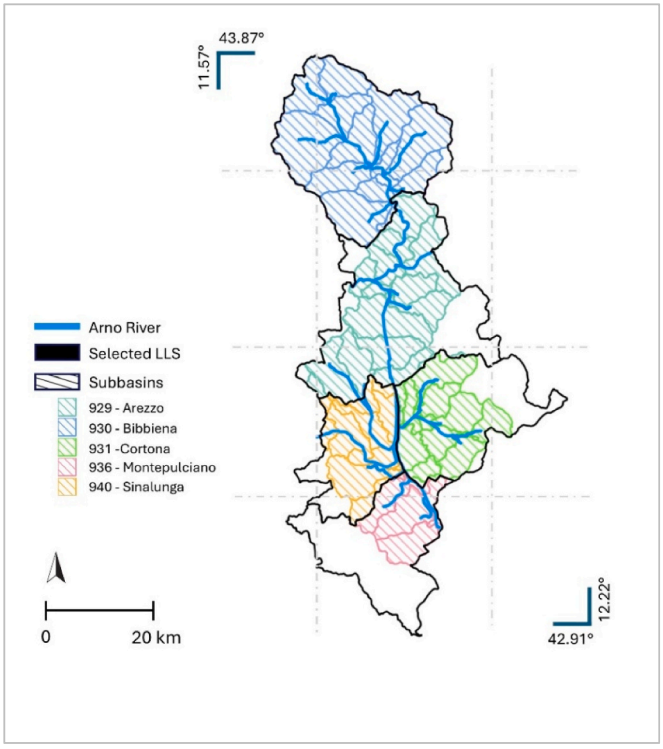

Source: Own elaboration

Fig. 3. Sub-basins associated with each of the five LLS.
Source: Own elaboration

2.4. Hydro-economic model

2.4.1. Environmentally extended MRIO model

The environmentally extended MRIO model (Miller and Blair, 2022) allows to calculate the total environmental resource *(E)* used by an economic system with *n* subregions and *m* industries:

$$E = C^T \cdot x \tag{1}$$

Where x is the *(mn x 1)* vector of outputs by economic sector and subregion and C is the *(mn x 1)* vector of environmental resource use intensities. T denotes the transpose.

The vector x can be expressed in function of the technical coefficients *(mn x mn)* matrix A and the *(mn x 1)* vector y of total final demand

$$x = (I - A)^{-1} \cdot y \tag{2}$$

Defining $L = (I - A)^{-1}$ as the multiregional Leontief inverse *(mn x mn)* matrix,

$$E = C^T \cdot L \cdot y \tag{3}$$

For the purposes of this study, the environmental resource is water. The extended water demand is defined as withdrawals (blue and green water) minus discharges plus the water requirements for dilution (grey water).

The extended demand of water *(m x 1)* vector for each subregion $\left(e_k^s\right)$ could be expressed as:

$$e_k^s = \left(\widehat{f_k^s} - \widehat{r_k^s} + \widehat{w_k^s}\right) \cdot L^s \cdot y \tag{4}$$

Where the L^s *(m x mn)* matrix corresponds to the Leontief inverse matrix blocks associated with production in the subregion *s*, y *(mn x 1)* vector is the final demand and f_k^s, r_k^s and correspond to the *(m x 1)* vectors (in $m^3/€$) of intensity coefficients for withdrawals, discharges and water for dilution, respectively, by water body k (groundwater, surface water and soil moisture) in subregion s. The hat symbol indicates the diagonalization of the vector.

When hydrologic variability is considered, the water use coefficients change according to the hydrological components. Let us first define the water extended demand for the subregion *s* associated with water body *k*, industry *i* and year *t* (for notation simplicity we use x^s instead of $L^s y$):

$$e_{k,i,t}^s = \left(f_{k,i,t}^s - r_{k,i,t}^s + w_{k,i,t}^s\right) \cdot x_i^s \tag{5}$$

Withdrawal coefficients will change for agricultural sectors, due to variations in soil moisture availability, which will imply higher withdrawals from surface and groundwater bodies when demand for green water exceeds supply for agriculture. Discharge coefficients also change because withdrawing water from surface water and groundwater involves considering irrigation losses. The dilution water requirement coefficients will change for all sectors discharging polluted water, depending on runoff, groundwater recharge, which define the concentration of pollutant in the receiving bodies. The latter coefficients depend indirectly on soil moisture due to their estimation as a function of discharge volume.

The above will be explained and formalized in later sections, however, a general scheme for extended demand dependence in hydrology is

defined here.

Equations (6)–(8) present the water use coefficients, each of which can be written as a function of its deterministic value plus time-varying term, which depends on hydrological components:

$$f^s_{k,i,t} = \bar{f}^s_{k,i} + F^s_{k,i,t}\left(SM^s_t\right) \tag{6}$$

$$r^s_{k,i,t} = \bar{r}^s_{k,i} + R^s_{k,i,t}\left(SM^s_t\right) \tag{7}$$

$$w^s_{k,i,t} = \bar{w}^s_{k,i} + H^s_{k,i,t}\left[I^s_t, R^s_t, R^s_{k,i,t}\left(SM^s_t\right)\right] \tag{8}$$

Where I^s_t, R^s_t and SM^s_t are the groundwater recharge, the runoff and the soil moisture, respectively, in subregion s for year t, obtained with the hydrological model.

Using equations (6)–(8) it is possible to write a general form to the extend demand associated with the water body k, the industry i and the year t.

$$e^s_{k,i,t} = \bar{e}^s_{k,i} + \left[F^s_{k,i,t}\left(S^s_t\right) + R^s_{k,i,t}\left(S^s_t\right) + H_{k,i,t}\left[I^s_t, R^s_t, R_{k,i,t}\left(S^s_t\right)\right]\right]\cdot x^s_i \tag{9}$$

Note that $F^s_{k,i,t}\left(S^s_t\right) = 0$ and $R^s_{k,i,t}\left(S^s_t\right) = 0$ for non-agricultural sectors, and $H_{k,i,t}\left[I^s_t, R^s_t, R_{k,i,t}\left(S^s_t\right)\right] = 0$ for non-discharging sectors.

The following two subsections explain the dynamics of the water use intensity coefficients associated with the agricultural and discharging sectors.

2.4.2. Green-to-blue water substitution in agriculture

The withdrawal and discharge deterministic coefficients of the agricultural sectors can be broken down into the part requiring irrigation and the part associated with livestock (Rocchi et al., 2026; Sturla and Rocchi, 2024):

$$\bar{f}^s_{k,i} = \bar{f}^{s,irr}_{k,i} + \bar{f}^{s,liv}_{k,i} \tag{10}$$

$$\bar{r}^s_{k,i} = \bar{r}^{s,irr}_{k,i} + \bar{r}^{s,liv}_{k,i} \tag{11}$$

In this section, subscript i refers only to agricultural sectors.

The following expressions detail the methodology used to modify the water withdrawal and discharge coefficients for a given year, which is based on green water availability (soil moisture). This approach contrasts with previous studies that, due to the lack of physically based hydrological information, have used changes in precipitation and evapotranspiration as proxies for soil moisture (Rocchi et al., 2026; Sturla and Rocchi, 2024).

Let define $T^s_{i,t}$ as the additional groundwater and surface water withdrawals by the agricultural sector i, subregion s, year t, due to changes in soil moisture availability (SM^s). Then,

$$T^s_{i,t} = \begin{cases} \left(\bar{f}^{s,irr}_{sm,i}\cdot x^s_i - SM^s_t\right)\cdot\gamma \text{ if } S^s_t < \bar{f}^{irr}_{hc,i}\cdot x^s_i \\ 0 \text{ if } S^s_t \geq \bar{f}^{irr}_{hc,i}\cdot x^s_i \end{cases} \tag{12}$$

where,

$$\gamma^s_i = \frac{1}{1-\rho^s_i} \tag{13}$$

the parameter ρ^s_i corresponds to the losses associated with the irrigation process in region s and agricultural sector i. When irrigation is used to supply agricultural requirements, an additional water withdrawal due to irrigation efficiency must be considered.

The term $\bar{f}^{irr}_{hc,i}\cdot x^s_i$ corresponds to the water withdrawal from soil moisture on the average year (deterministic case).

To disaggregate the need for additional irrigation between groundwater and surface water, consider the following parameters:

δ^s_i: proportion of groundwater irrigation in sector i of subregion s

η^s_i: proportion of surface water irrigation in sector i of subregion $s$where,

$$\delta^s_i = \frac{\bar{f}^{s,irr}_{gw,i}}{\bar{f}^{s,irr}_{gw,i} + \bar{f}^{s,irr}_{sw,i}} \tag{14}$$

$$\eta^s_i = \frac{\bar{f}^{s,irr}_{sw,i}}{\bar{f}^{s,irr}_{gw,i} + \bar{f}^{s,irr}_{sw,i}} \tag{15}$$

Then, $T^s_{i,gw,t}$ and $T^s_{i,sw,t}$ correspond to the change in the withdrawals of groundwater and surface water in sector i for year t, respectively, due to the changes in soil moisture:

$$T^s_{i,gw,t} = \begin{cases} \delta^s_i\cdot\left(\bar{f}^{s,irr}_{sm,i}\cdot x^s_i - SM^s_t\right)\cdot\gamma^s_i \text{ if } S^s_t < \bar{f}^{irr}_{hc,i}\cdot x^s_i \\ 0 \text{ if } S^s_t \geq \bar{f}^{irr}_{hc,i}\cdot x^s_i \end{cases} \tag{16}$$

$$T^s_{i,sw,t} = \begin{cases} \eta^s_i\cdot\left(\bar{f}^{s,irr}_{sm,i}\cdot x^s_i - SM^s_t\right)\cdot\gamma^s_i \text{ if } S^s_t < \bar{f}^{irr}_{hc,i}\cdot x^s_i \\ 0 \text{ if } S^s_t \geq \bar{f}^{irr}_{hc,i}\cdot x^s_i \end{cases} \tag{17}$$

Adding the effect of soil moisture availability and dividing by x_i, yields the stochastic component of the withdrawal coefficient for groundwater and surface water in agricultural sectors:

$$F^s_{gw,i,t}\left(S^s_t\right) = \begin{cases} \dfrac{\delta^s_i\cdot\left(\bar{f}^{s,irr}_{sm,i}\cdot x^s_i - SM^s_t\right)\cdot\gamma^s_i}{x^s_i} & \text{if } S^s_t < \bar{f}^{irr}_{hc,i}\cdot x^s_i \\ 0 \text{ if } S^s_t \geq \bar{f}^{irr}_{hc,i}\cdot x^s_i \end{cases} \tag{18}$$

$$F^s_{sw,i,t}\left(S^s_t\right) = \begin{cases} \dfrac{\eta^s_i\cdot\left(\bar{f}^{s,irr}_{sm,i}\cdot x^s_i - SM^s_t\right)\cdot\gamma^s_i}{x^s_i} & \text{if } S^s_t < \bar{f}^{irr}_{hc,i}\cdot x^s_i \\ 0 \text{ if } S^s_t \geq \bar{f}^{irr}_{hc,i}\cdot x^s_i \end{cases} \tag{19}$$

For the withdrawal coefficient associated with soil moisture, its stochastic component is:

$$F^s_{sm,i,t}\left(S^s_t\right) = \begin{cases} \dfrac{SM^s_t - \bar{f}^{s,irr}_{sm,i}\cdot x^s_i}{x^s_i} \text{ if } S^s_t < \bar{f}^{irr}_{hc,i}\cdot x^s_i \\ 0 \text{ if } S^s_t \geq \bar{f}^{irr}_{hc,i}\cdot x^s_i \end{cases} \tag{20}$$

In this work it is assumed that discharges from the agricultural sector are entirely to groundwater. Considering α^s_i as the proportion of the discharged water with respect to the groundwater and surface water withdrawals for the agricultural sector i, it is obtained that the additional discharges due to hydrologic variability are:

$$R^s_{sm,i,t}\left(S^s_t\right) = \left[F^s_{gw,i,t}\left(S^s_t\right) + F^s_{sw,i,t}\left(S^s_t\right)\right]\cdot\alpha^s_i \tag{21}$$

$$R^s_{sm,i}\left(S^s_t\right) = 0 \tag{22}$$

where,

$$\alpha^s_i = \frac{\bar{r}^{s,irr}_{gw,i}}{\bar{f}^{s,irr}_{gw,i} + \bar{f}^{s,irr}_{sw,i}} \tag{23}$$

Since hydrologic variability influences only the withdrawal and discharge coefficients of the agricultural sectors, the above equations are sufficient to characterize equations (7) and (8) of the input-output model.

Note that parameters $\left(\delta^s_i, \eta^s_i, \alpha^s_i\right)$ are all defined based on the average hydrological condition, that is, for the deterministic situation. It is assumed an irrigation losses in groundwater and surface water equal to $\rho^s_i = 30\%$, obtaining $\gamma^s_i = 1.42$, for all agricultural sectors and subregions.

The irrigation loss parameter is assumed to be equal to 30% across all agricultural sectors and subregions, consistent with previous hydro-

economic applications for the Tuscany region (Rocchi et al., 2026). This assumption is adopted due to the lack of spatially explicit data on irrigation efficiency at the LLS level.

2.4.3. Water for dilution in discharging sectors

The deterministic coefficient $w^s_{k,i}$ of equation (5) was calculated by Rocchi et al. (2024) with a mixing model base on a mass balance of COD concentration with intermediate chemical reaction, improving the previous versions (Xie, 1996; Guan and Hubacek, 2008). For this study, the coefficient is calculated based on the same model, but considering time dependence and two endogenous effects:

- Discharges volumes from the agricultural sector depend on soil moisture availability, as discussed in the preceding section.
- The COD concentration in receiving water bodies depends on groundwater recharge (I_t) and runoff (R_t).

Details of the model used to calculate the water required for dilution, as well as the data used, are found in Appendix A.

2.5. Long-term natural supply

The long-term natural water supply is calculated based on the natural supply estimated using the SWAT model and an adjustment factor derived from historical precipitation data for the period 1971–2020 (Bartolini, 2014, 2018; SIR Toscana, 2021). This methodology allows for the correction of climatic biases present in the study period considered in this work (2005–2013).

Long-term groundwater recharge and surface runoff volumes are estimated as:

$$\overline{I}^s = \frac{\tau^s}{T}\sum_{t=1}^{T} I^s_t \tag{24}$$

$$\overline{R}^s = \frac{\tau^s}{T}\sum_{t=1}^{T} R^s_t \tag{25}$$

Where τ^s corresponds to a bias correction factor for the analysis period calculated on the basis of the precipitation for a longer period (T^*, $1971-2020$) and the precipitation for the analysis period (T).

$$\tau^s = \frac{\frac{1}{T^*}\sum_{t=1}^{T^*} P^s_t}{\frac{1}{T}\sum_{t=1}^{T} P^s_t} \tag{26}$$

2.6. Natural ecological supply and feasible supply

Natural ecological supply (ES) refers to the long-term natural water supply net of the ecological flow requirement.

$$ES^s = \overline{I}^s + (1-E)\overline{R}^s \tag{27}$$

The estimation of feasible water supply follows the methodology proposed by Rocchi et al. (2024), which incorporates environmental, institutional, and technical constraints into the natural supply of surface and groundwater.

$$I^{s,feas}_t = \left\{ \begin{array}{c} \overline{I}^s(1-B^s)\ if\ I^s_t < \overline{I}^s(1-B^s) \\ \overline{I}^s(1+B^sB)\ if\ I^s_t > \overline{I}^s(1+B^s) \\ I^s_t\ if\ I^s_t \in [\overline{I}^s(1-B^s), \overline{I}^s(1+B^s)] \end{array} \right\} \tag{28}$$

$$R^{s,feas}_t = \left\{ \begin{array}{c} R^s_t - E\overline{R}^s\ if\ E\overline{R}^s \le R^s_t \le M^s\overline{R}^s + E\overline{R}^s \\ M^s\overline{R}^s\ if\ R^s_t > M^s\overline{R}^s + E\overline{R}^s \\ 0\ if\ R^s_t < E\overline{R}^s \end{array} \right\} \tag{29}$$

where,

I^s_t: Groundwater recharge volume in year t in subregion s
$\overline{I}^s$: Long-term groundwater recharge volume in subregion s
B^s: Parameter defining the range of groundwater feasible availability in subregion s
R^s_t: Runoff volume in year t (multivariate model)
$\overline{R}^s$: Long-term runoff volume in subregion s
E: Ecological flow as proportion of mean runoff
M^s: Maximum volume of concessions as proportion of mean runoff in subregion s

An environmental flow of 20% is considered for surface water (Rossi and Caporali, 2010), a depletion threshold of 13% for groundwater (Rocchi et al., 2024). In this case, the Maximum Volume of Concessions as a Proportion of Mean Runoff is set to 1, since no external water concessions are considered; the analysis is restricted to water naturally generated within the basin, along with transfers from the Montedoglio reservoir— in contrast to Rocchi et al. (2026) who consider surface water supply based on concession volumes.

2.7. Green water supply

Green water supply is estimated based on Soil Moisture (SM) and Evapotranspiration (ET) (Pacetti et al., 2021). However, since this study focuses on green water availability for the agricultural sector during the irrigation period, two adjustment factors are applied: the percentage of agricultural area in each LLS (β^s_A) and the number of months in the year when irrigation takes place (5 month).

Accordingly, the indicator of water availability is defined as:

$$GWA^s = (ET^s + SM^s)\cdot\beta^s_A\cdot\frac{5}{12} \tag{30}$$

2.8. Scarcity indicators

The following water scarcity indicators will be used to characterize the LLS.

2.8.1. WEI

The WEI corresponds to the ratio between blue water withdrawals of groundwater and surface water, and the long term natural availability net of the ecological flow (natural ecological supply, ES) (European Environment Agency, 2020).

$$WEI_t = \frac{\sum_{i=1}^{N}\sum_{k=1}^{2} f^s_{k,i,t}\cdot x^s_i}{ES^s} \tag{31}$$

2.8.2. WEI$^+$

The WEI$^+$, is an upgraded version of the WEI, which incorporates returns from water uses, therefore taking into account the net water demand (Faergemann, 2012; European Environmental Agency, 2020)

$$WEI^+_t = \frac{\sum_{i=1}^{N}\sum_{k=1}^{2}\left(f^s_{k,i,t} - r^s_{k,i,t}\right)\cdot x^s_i}{ES^s} \tag{32}$$

2.8.3. EWEI

The EWEI indicator is estimated as the extended water demand

divided by the feasible supply (Rocchi et al., 2026).

$$EWEI_t = \frac{\sum_{i=1}^{N}\sum_{k=1}^{2}\left(f^s_{k,i,t} - r^s_{k,i,t} + w^s_{k,i,t}\right)\cdot x^s_i}{I^{s,feas}_t + R^{s,feas}_t} \quad (33)$$

2.8.4. EWEI*

The EWEI* indicator corresponds to the EWEI calculated using the natural ecological supply in the year of analysis, rather than in the long term. It is defined as the groundwater recharge and surface runoff, minus the ecological flow. This indicator is proposed in the present study.

$$EWEI^{*s}_t = \frac{\sum_{i=1}^{N}\sum_{k=1}^{2}\left(f^s_{k,i,t} - r^s_{k,i,t} + w^s_{k,i,t}\right)\cdot x^s_i}{I^s_t + R^s_t - \overline{ER}^s} \quad (34)$$

2.8.5. GWSI

The green water scarcity index (GWSI) is derived based on agricultural soil moisture demand and green water supply. v

$$GWSI^s_t = \frac{\sum_{i=1}^{N} f^s_{sm,i,t}\cdot x^s_i}{GWA^s_t} \quad (35)$$

This formulation captures the effective green water available for the agricultural sector, rather than total soil moisture, thereby ensuring consistency with sectoral water requirements. In Equation (35), the numerator explicitly represents the *implicit green water demand associated with actual economic output*, while the denominator corresponds to the *effective green water availability* for the agricultural sector, as previously defined in Equation (30). This definition distinguishes the proposed Green Water Scarcity Index (GWSI) from conventional accounting approaches based solely on land cover area, by directly linking water use to production dynamics rather than spatial proxies. Explicitly accounting for green water availability is essential for capturing the dynamics of water demand in the agricultural sector. In particular, it enables a physically grounded characterization of the substitution between green and blue water, whereby deficits in soil moisture trigger additional withdrawals from surface and groundwater sources. Previous studies have approximated this mechanism using proxies such as precipitation or evapotranspiration (Sturla and Rocchi, 2024; Rocchi et al., 2026), which do not fully capture the underlying hydrological processes.

More broadly, this approach is consistent with the literature recognizing that both blue water (surface and groundwater) and green water (soil moisture) constitute fundamental components of water availability, especially in agricultural systems (Chapagain and Hoekstra, 2004; Rijsberman, 2006; Zhao et al., 2011). By incorporating soil moisture as a physically based variable, the GWSI provides a more realistic and internally consistent representation of water scarcity conditions affecting agricultural production.

This study considers the standard scarcity threshold values, 20% for scarcity and 40% for severe scarcity (OECD, 2015; Pfister et al., 2009).

2.9. Data

The input data for the SWAT model—including precipitation, temperature, solar radiation, relative humidity, and other climatic variables—were obtained from Braca et al. (2021, 2022), Sir Toscana (2021), and ISTAT (2021).

The intensity coefficients for blue and green water use were sourced from the study by Rocchi et al. (2026). For water quality parameters related to effluent discharges (COD), legally permitted maximum values were used, based on ISTAT (2019). COD concentrations were assigned to discharges from the main macro-sectors (agriculture, manufacturing, and sewerage), following sector-specific characterization approaches. The parameters governing pollutant dynamics in the mixing model—namely the reaction rate after discharge and the purification rate prior to entering water bodies—were taken from Guan and Hubacek (2008), ensuring consistency with established hydro-economic modeling practices. The standard COD concentration in receiving water bodies was set at 20 mg/L, corresponding to unpolluted conditions (Rossi and Benedini, 2020), and was adjusted within a plausible range under wet and dry conditions. While these parameters are not locally calibrated due to data limitations, they are grounded in the literature and selected to ensure internal consistency and numerical stability of the model. In addition, the relationship between water quality and hydrological availability was parameterized following Rocchi et al. (2024), allowing COD concentrations to vary consistently with changes in runoff and groundwater recharge.

The thresholds for moderate and severe water scarcity indicators were obtained from the European Environmental Agency (2020), with values of 0.2 and 0.4, respectively.

The MRIO table used in this study (Fig. 4) was developed by the Tuscan Regional Institute for Economic Planning (IRPET, 2021). The original table included agriculture as a single industry. The final multi-regional matrix is referred to year 2017 and contains 53 economic sectors, 49 LLSs, 5 components of the internal final demand and 4 components of external final demand (Rest of Italy and Rest of the World).

All other data sources have been described in the previous sections an.

3. Results

3.1. Hydrological results

Table 2 presents the results of the hydrological model by LLS and year, which are used in this study to estimate both water supply and demand in their various forms. Fig. 5 shows the average natural supply of groundwater (recharge) and surface water (runoff) by LLS, as well as the green water supply, estimated as the soil moisture in agricultural areas during the irrigation months.

3.2. Water demand

Water demand by LLS has been estimated based on the interaction between the MRIO model and the hydrological model. Four types of demand have been characterized: Water Withdrawals (WD), Net Demand or blue water (ND), Extended Demand, which includes blue and grey water (ED), and Green water Demand (GD). All demand types show year-to-year variability, largely driven by the substitution between green and blue water in agriculture when natural water availability is insufficient. In some areas this substitution is observed, while in others no shortage occurs. Environmental demand also varies over time, reflecting the dependence of water quality requirements on overall supply conditions. Table 3 presents these patterns by LLS and year.

3.3. Scarcity indicators

Fig. 6 shows the temporal evolution of the four indicators related to blue and grey water (WEI, WEI+, EWEI, EWEI*) in the LLSs considered. These figures include the thresholds for moderate (0.2) and severe (0.4) water scarcity. In addition, the EWEI obtained in the study by Rocchi et al. (2026) is included for comparison.

The results show that in Arezzo, scarcity remained limited: only in one year did the enhanced index (EWEI*) rise above the moderate threshold, while all other indicators stayed below. Bibbiena shows an even more stable picture, with none of the indicators surpassing the moderate threshold.

Cortona displayed the most critical pattern. Here, the WEI exceeded the severe threshold in three years, the EWEI* in two years, and the EWEI in three years, pointing to recurrent high stress conditions.

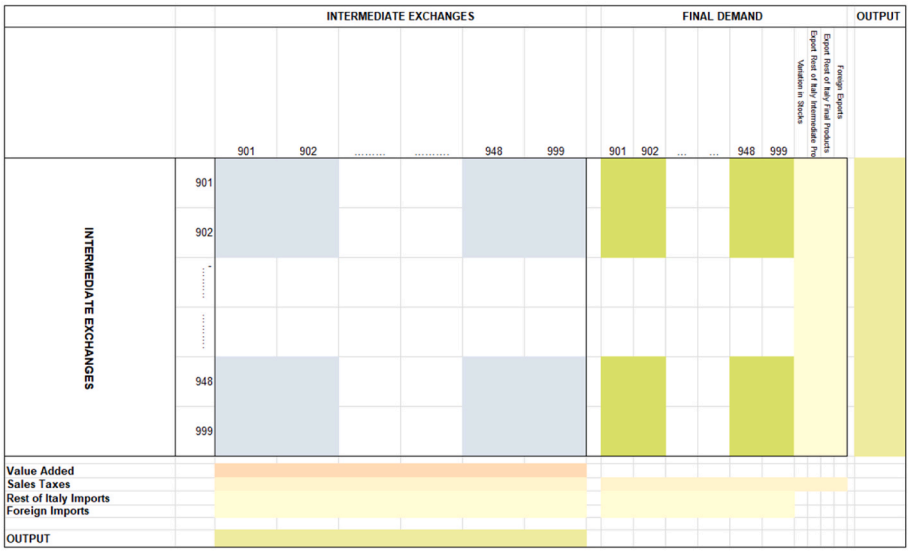

Source: Own elaboration based on IRPET (2021)

Fig. 4. Structure of the IRIO table of Tuscany.
Source: Own elaboration based on IRPET (2021).

Table 2
Hydrological results by LLS and year.

LLS	Year	Precipitation [Mm3]	Evapotranspiration [Mm3]	Groundwater Recharge [Mm3]	Surface Runoff [Mm3]	Soil Moisture [Mm3]	Green Water Supply [Mm3]
Arezzo	2014	686.9	396.0	178.9	93.5	80.0	73.4
	2015	552.1	410.1	99.2	74.3	68.1	73.7
	2016	856.6	422.8	217.7	153.2	78.7	77.3
	2017	487.5	343.6	91.0	54.1	63.4	62.7
	2018	735.1	365.9	212.3	116.2	71.7	67.4
	2019	805.3	373.6	214.0	183.2	82.9	70.4
	2020	655.1	366.3	155.7	106.0	76.1	68.2
Bibbiena	2014	902.8	333.0	321.5	199.4	81.4	29.4
	2015	568.2	356.1	136.3	82.5	67.4	30.0
	2016	881.7	357.7	285.9	188.5	78.9	30.9
	2017	575.8	342.6	127.2	76.1	62.1	28.7
	2018	897.5	326.0	319.3	207.3	79.8	28.7
	2019	983.9	328.7	310.1	298.2	81.4	29.0
	2020	820.8	335.5	238.5	159.4	78.7	29.3
Cortona	2014	414.5	259.6	82.8	54.8	58.5	68.9
	2015	283.8	249.6	30.9	45.9	45.2	63.9
	2016	489.2	281.8	83.4	74.0	58.3	73.7
	2017	338.9	247.1	53.1	45.6	45.9	63.5
	2018	434.7	241.8	80.4	84.0	51.9	63.6
	2019	371.2	235.9	59.1	60.8	57.3	63.5
	2020	308.1	205.8	68.9	37.8	48.1	55.0
Montepulciano	2014	368.9	240.9	46.2	62.7	71.1	84.5
	2015	259.9	246.1	17.9	46.8	54.8	81.5
	2016	439.6	267.3	37.0	88.3	68.0	90.8
	2017	159.6	178.9	6.4	7.9	46.0	60.9
	2018	434.0	231.1	46.6	111.7	59.7	78.8
	2019	424.3	224.0	54.3	127.5	71.0	79.9
	2020	291.0	221.7	27.6	38.7	67.9	78.4
Sinalunga	2014	270.6	175.3	50.2	33.4	44.9	56.9
	2015	205.5	179.9	25.7	30.6	35.8	55.7
	2016	338.8	190.8	55.4	59.4	43.6	60.6
	2017	133.4	134.5	11.9	7.3	31.4	42.8
	2018	305.5	163.6	55.6	58.8	37.7	52.0
	2019	324.7	159.3	72.3	82.7	44.7	52.7
	2020	226.0	160.1	33.5	25.7	42.3	52.3

Source: Own elaboration

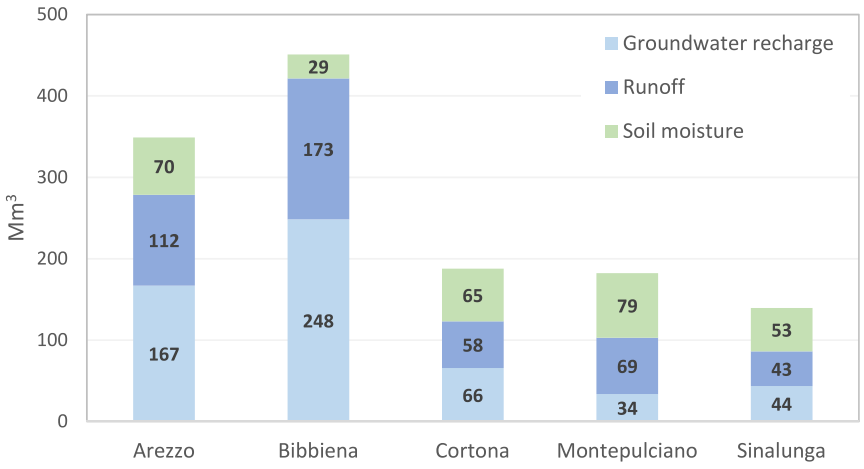

Source: Own elaboration

Fig. 5. Natural supply by LLS. Blue water (groundwater recharge and runoff) and green water (soil moisture).
Source: Own elaboration

Table 3
Water demand by LLS and year.

LLS	Demand Category	2014	2015	2016	2017	2018	2019	2020
Arezzo	WD	23.8	23.8	23.8	23.8	23.8	23.8	23.8
	ND	8.5	8.5	8.5	8.5	8.5	8.5	8.5
	GD	57.9	57.9	57.9	57.9	57.9	57.9	57.9
	ED	30.3	29.7	26.9	29.1	30.3	25.8	30.8
Bibbiena	WD	6.4	6.4	6.4	6.4	6.4	6.4	6.4
	ND	2.7	2.7	2.7	2.7	2.7	2.7	2.7
	GD	26.1	26.1	26.1	26.1	26.1	26.1	26.1
	ED	9.0	9.0	9.2	9.0	8.9	8.0	9.5
Cortona	WD	30.2	49.2	30.6	48.3	39.7	32.0	45.1
	ND	19.5	33.2	19.7	32.5	26.4	20.8	30.2
	GD	65.4	65.4	65.4	65.4	65.4	65.4	65.4
	ED	30.9	47.4	29.9	47.1	37.3	33.0	44.1
Montepulciano	WD	6.3	6.3	6.3	16.2	6.3	6.3	6.3
	ND	3.5	3.5	3.5	11.4	3.5	3.5	3.5
	GD	79.0	79.0	79.0	79.0	79.0	79.0	79.0
	ED	7.5	7.5	7.2	16.3	6.7	6.7	7.5
Sinalunga	WD	10.6	23.6	12.4	30.0	20.9	10.9	14.4
	ND	5.4	13.9	6.6	18.1	12.1	5.6	7.9
	GD	51.9	51.9	51.9	51.9	51.9	51.9	51.9
	ED	12.7	23.5	13.1	28.5	20.0	11.4	15.7

Source: Own elaboration

In Montepulciano, only the EWEI crossed the scarcity thresholds, indicating severe scarcity in one year.

Sinalunga revealed intermittent stress: the EWEI* exceeded the severe threshold in two years, the EWEI did so in one year, and other indicators rose above the moderate threshold at least once.

Fig. 7 presents the Green Water Scarcity Indicator (GWSI) proposed in this study for all LLS. This indicator reflects situations in which a green water deficit occurs and must be compensated by blue water. Over the study period, no green water deficit was recorded in either Arezzo or Bibbiena. In contrast, Cortona experienced frequent shortages, with deficits occurring in five out of the seven simulated years. Montepulciano showed a pronounced deficit in one particular year, while Sinalunga registered a deficit only once.

A sensitivity analysis of the irrigation loss rate (ρ) was conducted (see Appendix B). Results indicate that variations between 20% and 40% lead to significant changes in water demand and water scarcity indicators, confirming the strong influence of irrigation efficiency on model outcomes.

4. Discussion

4.1. Result analysis

The results show contrasting conditions across the study areas. Arezzo and Bibbiena stand out for their stability: no green water deficits were recorded, and all scarcity indicators remained below critical thresholds. These findings are consistent with the estimates of Rocchi et al. (2026), confirming the absence of significant water scarcity in these locations.

By contrast, Cortona presents the most critical situation. Here,

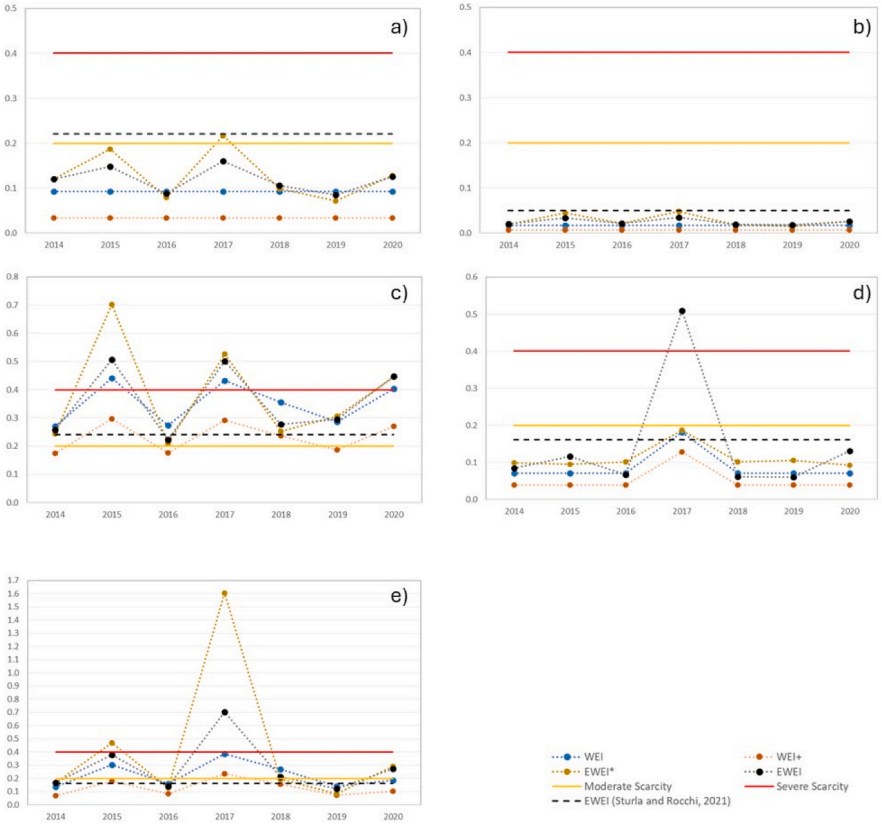

Source: Own elaboration

Fig. 6. Blue and grey water scarcity indicators (a = Arezzo, b = Bibbiena, c = Cortona, d = Montepulciano, e = Sinalunga).
Source: Own elaboration

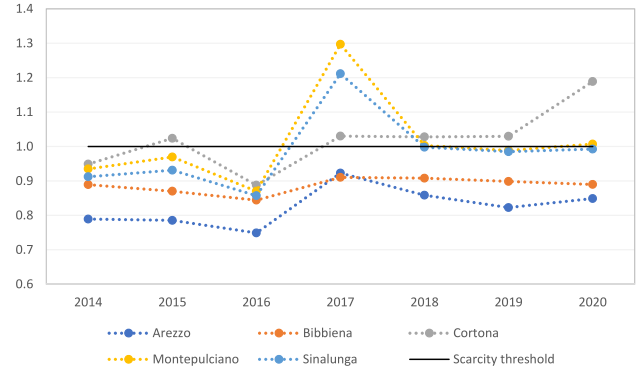

Source: Own elaboration

Fig. 7. Green water scarcity indicator (All LLS).
Source: Own elaboration

frequent green water deficits coincide with multiple years in which scarcity indicators exceed the severe threshold, revealing a persistent pattern of stress. This outcome is more severe than the moderate scarcity reported by Sturla and Rocchi et al. (2026). Montepulciano shows occasional scarcity, with one year marked by both a pronounced green water deficit and a severe EWEI value. Sinalunga, too, displays intermittent stress: thresholds are exceeded in some years, and a green water deficit occurs once. While less consistent than Cortona, these results highlight notable vulnerability.

Taken together, the findings point to significant water scarcity in Cortona, Montepulciano, and Sinalunga, with Cortona and Sinalunga emerging as the most critical cases. Severe scarcity is primarily detected by the EWEI* and EWEI indicators, which account for grey water. During the most critical years, limited blue water availability and green water deficits jointly increase pressure: reduced surface water decreases the dilution capacity for pollutants, raising grey water requirements, while agriculture relies more heavily on blue water to compensate for missing green water. The GWSI introduced in this study captures these interactions explicitly, highlighting the years and locations where green water shortages triggered substitution with blue water and exacerbated overall scarcity conditions.

The results should be interpreted considering that the economic structure is held constant (2017), while hydrological conditions vary over the period 2014–2020. This approach allows isolating the effect of hydrological variability on water scarcity indicators, avoiding confounding effects from structural economic changes. Importantly, despite the static production structure, the model captures endogenous dynamics in water demand, as water use responds directly to hydrological conditions. In particular, the substitution between green and blue water in agriculture, as well as variations in grey water requirements in discharging sectors, are driven by changes in soil moisture, runoff, and groundwater recharge. As a result, the variability observed across years reflects hydrologically induced adjustments in water demand, providing a consistent basis for comparing local vulnerabilities under different hydrological conditions. Therefore, the results remain robust and relevant, as they capture the response of the economic system to realistic hydrological variability, which is a key driver of water scarcity in the study area.

4.2. *Theoretical and practical contributions*

The present study advances the field by explicitly incorporating a green water scarcity indicator together with a physically based mechanism for green-to-blue water substitution in agriculture. This integrated

approach enables a more realistic assessment of future water stress scenarios under climate change, thereby offering critical insights for the formulation of adaptive and sustainable water policies at the local level.

Specifically, the principal advantages of this approach relative to prior models are threefold: (i) greater accuracy in estimating key hydrological components—including precipitation, evapotranspiration, surface runoff, groundwater recharge, and soil moisture; (ii) the estimation of surface runoff under natural (unregulated) conditions, enabling a more precise assessment of natural water availability and, in turn, improving scarcity metrics while refining grey-water estimates via the mixing model; and (iii) the explicit representation of soil moisture, which permits the quantification of green-water supply for agriculture and a more realistic simulation of increased surface- and groundwater withdrawals during deficit years.

Indeed, using multidimensional water scarcity indicators (blue, grey, and green water) provides a valuable basis for informed local decision-making in water management (European Environment Agency, 2020; UN WWDR, 2024). Of particular importance is the use of blue water by agriculture, which places additional pressure on both surface and groundwater ecosystems, especially when soil moisture levels are low. This phenomenon has been largely understudied in hydro-economic models, or addressed only through simplified approximations (Rocchi et al., 2026). Climate change impacts in Tuscany include a reduction in precipitation and an increase in evapotranspiration (D'Oria et al., 2019; Bartolini et al., 2017; Pranzine et al., 2020) strongly affecting water related ecosystem services (El Jeitany et al., 2024a). These changes are expected to decrease the availability of both blue and green water (i.e., soil moisture), increasing the reliance of agricultural systems on blue water sources (Baggio et al., 2021). Understanding this substitution dynamic is essential for the design of effective mitigation strategies. The present study contributes to this goal by explicitly incorporating a green water scarcity indicator and a physically based mechanism for green-to-blue water substitution in agriculture. This integrated approach allows for a more realistic assessment of future water stress scenarios under climate change, offering critical insights for the formulation of adaptive and sustainable water policies at the local level.

4.3. Limitations and future work

This study relies on exogenous scarcity thresholds, which could be endogenously defined in future research by incorporating intra-annual variability in both water supply and demand. Moreover, the spatial scope is limited to a subset of the Tuscany region, which constrains the regional-scale analysis of water scarcity and the design of coherent public policies. Future research should expand hydrological modeling to include the remaining river basins in the region. This extension would also enable the use of the MRIO model to assess virtual water flows among Tuscany's local economies, providing valuable insights into water use and governance.

Another important aspect to consider is the distortion generated by water concessions. This study has assessed water availability under natural conditions—something that models lacking a physical basis cannot adequately capture. However, the characterization of scarcity could be improved by incorporating water concessions in each local economy, as well as downstream commitments (Venturi et al., 2014; Rocchi et al., 2024; 2026). A given LLS might show favorable scarcity indicators, but still face difficulties if required to allow water to flow downstream. This institutional dimension represents a key challenge for future research, and may also be highly relevant for improving the management of water rights allocation or reallocation, taking into account the hydrological, productive, and institutional structure of the territory.

The study assumes a static production structure and represents hydrological variability over the SWAT modelling period (2014–2020). The former limitation reflects the difficulty of constructing an economic characterization at such fine spatial resolution; nevertheless, forward-looking projections are feasible. Regarding future hydrological conditions, an important extension is to integrate temperature and precipitation information for climate-change analysis under alternative socioeconomic scenarios (IPCC et al., 2021), enabling the projection of indicators while holding the current production structure constant. Coupling this with economic projections would yield a more realistic depiction of the temporal evolution of the indicators at the LLS scale through, for example, 2050.

Although the proposed framework provides a detailed and physically grounded representation of hydrological–economic interactions, future research should incorporate systematic benchmarking against widely used integrated tools such as WEAP and similar hydro-economic models. Such comparisons would allow for a more comprehensive evaluation of model performance, including differences in hydrological representation, scenario sensitivity, and policy relevance. In particular, benchmarking exercises could help identify the added value of process-based approaches like SWAT in capturing green–blue water dynamics, while also assessing the trade-offs in terms of data requirements and computational complexity. This would ultimately strengthen the robustness of the framework and enhance its credibility and applicability in decision-making contexts.

The assumption of uniform irrigation losses across sectors and sub-regions represents a simplification that may not fully capture spatial heterogeneity in irrigation efficiency. In this study, a homogeneous irrigation loss rate ($\rho = 30\%$) was adopted, consistent with estimates for the Tuscany region (Rocchi et al., 2024, 2026), due to the lack of detailed information at the Local Labor System (LLS) level. However, irrigation losses are influenced by factors such as infrastructure, conveyance systems, and management practices, which can vary significantly across locations. The sensitivity analysis conducted for the water-stressed case of Cortona confirms that this parameter is a key driver of both water demand and water scarcity indicators. Variations in ρ between 20% and 40% lead to significant changes in water demand (around $\pm$8–11%) and in scarcity indicators. In particular, WEI shows higher sensitivity than WEI+, as it is based on gross demand, while WEI + partially mitigates this effect by considering net demand. Likewise, EWEI and EWEI* exhibit lower variability due to the inclusion of extended demand (net demand plus grey water), which reduces the relative impact of irrigation losses; both indicators respond similarly because only their denominator differs. As expected, green water-based indicators remain unaffected. Importantly, higher irrigation losses increase the reliance on blue water to meet agricultural needs, reinforcing the substitution of green water by blue water due to inefficiencies in water delivery and application. Given the magnitude of these effects, the results highlight that irrigation losses are not only a critical but also a highly sensitive parameter in water scarcity assessments. Therefore, improving the estimation of irrigation loss rates at the local economy level is essential to enhance the robustness and reliability of the results.

With respect to the representation of agricultural responses to water scarcity, the framework does not incorporate dynamic feedback mechanisms, as the unidirectional data transfer structure implies fixed technical coefficients for water use, meaning that blue water withdrawals adjust proportionally to output. As a result, it does not capture adaptive responses such as crop switching, fallowing, adjustments in irrigation practices, or even reductions in production under severe drought conditions. This assumption may lead to an overestimation of water demand under scarcity, as it does not account for producers' ability to adapt to hydrological constraints. This reflects a broader limitation of input–output models, which, while enabling a transparent integration of hydrological processes, do not incorporate behavioral responses or elasticities, in contrast to computable general equilibrium models (Rocchi et al., 2026). Nevertheless, future research could address this limitation by incorporating elasticity-based adjustments in the agricultural sector, allowing water-use coefficients to respond to hydrological conditions.

An additional limitation relates to the temporal resolution of the

model. The framework operates at an annual scale, which may smooth intra-annual variability in water availability and demand. This is particularly relevant in Mediterranean climates, such as that of the Tuscany region in Italy, where precipitation is highly seasonal and peak agricultural water demand occurs during the dry summer period (Sturla and Rocchi, 2024). It is important to note that, from a hydrological perspective, the SWAT model is implemented at a monthly scale; however, its integration with the economic MRIO model requires aggregation to an annual scale, thereby limiting the ability to capture intra-annual dynamics. As a result, annual indicators may underestimate short-term imbalances between water supply and demand. Future research should consider the incorporation of monthly or seasonal temporal resolutions or, alternatively, as proposed by Rocchi et al. (2026), the estimation of scarcity thresholds that can be compared with the indicators—representing an additional refinement of the model—and that explicitly incorporate the seasonal variability of water supply and demand, using seasonal irrigation water use profiles.

Furthermore, future research should also consider the interaction between landscape configuration, hydrological modeling, and ecosystem services, as spatial patterns of land use directly influence water availability and regulation. Incorporating this dimension would improve the ecological realism of scarcity assessments and highlight synergies and trade-offs between water use, agricultural productivity, and ecosystem service provision (Jeitany et al., 2024b).

Finally, such an approach would also allow for the estimation of the water footprint of each LLS, adjusted by scarcity and incorporating social criteria, such as the local capacity for socio-institutional water governance (Sturla et al., 2023; Wichelns, 2017; Wang et al., 2021; Pfister et al., 2009).

4.4. Policy implications

The results support a set of concrete and operational policy instruments for water management at the local and basin scales. First, allocation rules could be designed to link seasonal caps on blue-water withdrawals to observed scarcity indicators and soil-moisture anomalies. In LLS where indicators such as EWEI* or GWSI exceed critical thresholds—particularly in Cortona, Montepulciano, and Sinalunga—adaptive measures such as temporary curtailments and ecological-flow safeguards could be implemented during consecutive dry periods. This type of adaptive allocation is consistent with integrated river basin management approaches promoted in the study area (Northern Apennine District Authority, 2021).

Second, the framework enables the evaluation of infrastructure and nature-based solutions under different hydrological conditions. By incorporating climate-change projections and socioeconomic scenarios, policymakers could assess investments in conjunctive-use systems, managed aquifer recharge, leakage reduction, and riparian restoration, with the objective of increasing infiltration, reducing losses, and stabilizing water availability during low-flow periods. These interventions are particularly relevant in territories with recurrent green water deficits, where pressure on blue water resources intensifies.

Third, the indicators provide a basis for economic instruments that reflect both quantity and quality dimensions of water use. These include scarcity-adjusted volumetric charges on blue water during green-water deficits, grey-water fees linked to dilution requirements in areas with limited assimilative capacity, and payments for ecosystem services in priority recharge zones, with rates informed by the marginal value of water within the system (Pacetti et al., 2026).

Fourth, the observed spatial heterogeneity in water scarcity suggests that policy measures should be territorially differentiated. Rather than uniform regional policies, targeted interventions in the most critical LLS could yield higher efficiency gains. This territorial perspective is aligned with the literature emphasizing the need for water governance at the local scale, where hydrological conditions and socio-economic structures interact more directly (Rossi and Benedini, 2020). In contexts of severe scarcity—potentially associated with output losses—policy responses could extend beyond efficiency improvements to include adjustments in water rights allocation and sectoral rebalancing of water use.

Importantly, while the present analysis is based on observed hydrological variability, the modeling framework is readily extendable to scenario analysis. This includes the evaluation of drought conditions, changes in production structure, and the adoption of water-saving technologies, thereby supporting forward-looking and adaptive policy design.

Crucially, these policy applications are enabled by the model's capacity to integrate economic and hydrological scales—linking local economies with basins and sub-basins—thereby providing spatially consistent attribution, constraints, and counterfactual analysis across scales.

These implications should be interpreted in light of the analytical scale adopted. Although LLS are not formal governance units, their coherent aggregation to sub-basin and basin levels (Pacetti et al., 2026) enables direct translation into river basin management plans and regional policy instruments (D'Oria et al., 2019; Fatichi and Caporali, 2009). The contribution of the framework lies not in redefining governance boundaries, but in providing granular evidence on intra-regional redistribution of pressure, stress, and impact-based risk that can be incorporated into existing planning and regulatory processes.

5. Conclusions

This study addresses a key gap in the literature on environmentally extended input–output models by harmonizing hydrological and economic spatial scales. This is achieved by aggregating sub-basins according to local economies (LLS), enabling the estimation of natural water supply—both blue and green—within local economies using the physically based SWAT model. Green water availability, often omitted in previous MRIO applications, is explicitly considered. The interaction between the SWAT model and the hydro-economic MRIO model facilitates the estimation of blue, grey, and green water demand, as well as both natural and feasible water supply.

The integrated model is applied to five local economies in the upper Arno River basin, Tuscany, Italy. Based on this framework, five water scarcity indicators are constructed (WEI, WEI+, EWEI*, EWEI, and GWSI), two of which—EWEI* and GWSI—are proposed in this study. These indicators enable a nuanced assessment of water scarcity that captures the complex interactions between water availability, pollution loads, and sectoral water demand.

In contrast to previous MRIO-based approaches, this study provides a spatially and physically grounded estimation of both blue and green water supply at the sub-basin level. The inclusion of green water supply allows for the explicit simulation of the green-to-blue water substitution process in agriculture—an essential yet often overlooked mechanism that directly affects blue water scarcity indicators. This represents a substantial advancement over earlier studies which relied on precipitation as a proxy for soil moisture.

The results reveal that three of the five LLS (Cortona, Montepulciano, and Sinalunga) experience green water scarcity in some years, which in turn increases pressure on blue water resources. While Arezzo and Bibbiena show minimal signs of water stress, the other three LLS face episodes of severe scarcity—particularly when evaluated using the EWEI* and EWEI indicators. These metrics, by incorporating both grey water requirements and constrained supply conditions, offer a more realistic picture of water scarcity. Notably, EWEI*, although based on a higher water availability estimate, can in some years exceed EWEI due to its lack of consideration for groundwater storage dynamics.

Additionally, although this study does not explicitly calculate virtual water flows—either in volumetric or scarcity-weighted terms—the proposed model offers a unique advantage for their assessment and for identifying indirect pressure transfers across cross-regional supply

chains. This advantage stems from the coherent integration of hydrological and economic scales, by combining a physically based hydrological model with an economic MRIO framework. This integration provides a robust basis for characterizing both blue and green water supply, as well as the variability of water demand, driven not only by grey water requirements—conditioned by hydrological availability—but also by the explicit estimation of green water scarcity and the simulation of green-to-blue water substitution in agriculture, both absent in conventional water footprint approaches. Furthermore, for scarcity-weighted virtual water flows—an emerging research area—the study offers a set of indicators that can support their estimation.

In conclusion, this study makes a significant methodological and applied contribution. By integrating hydrological and economic dimensions within a coherent framework, it enables a more realistic representation of water scarcity dynamics, including the substitution between green and blue water in agriculture and the reduced assimilative capacity of water bodies during dry periods. Additionally, the development and comparison of both existing and novel indicators allow for a more comprehensive and multidimensional characterization of water scarcity (blue, grey and green water). In this context, the framework also provides a consistent basis for future analyses of virtual water flows and their associated scarcity-related pressures. This approach offers valuable insights for future research and policy design aimed at improving local water resource management under increasing climatic and economic pressures.

CRediT authorship contribution statement

Gino Sturla: Writing – review & editing, Writing – original draft, Visualization, Validation, Software, Resources, Methodology, Investigation, Formal analysis, Data curation, Conceptualization. **Benedetto Rocchi:** Writing – review & editing, Validation, Supervision, Project administration, Funding acquisition, Conceptualization. **Enrica Caporali:** Writing – review & editing, Validation, Supervision, Conceptualization. **Tommaso Pacetti:** Writing – review & editing, Writing – original draft, Visualization, Validation, Software, Methodology, Investigation, Formal analysis, Data curation, Conceptualization.

Declaration of competing interest

The authors declare that they have no known competing financial interests or personal relationships that could have appeared to influence the work reported in this paper.

Appendices. 7

7.1 Appendix A. Water for dilution

The coefficients of water requirements for dilution by water body k and industry I for the year t, is expressed as:

$$w^s_{k,i,t} = \frac{u^s_{k,i,t}}{x^s_i} \tag{A.1}$$

Where, $u^s_{k,i,t}$ (m^3/year) is the water for dilution, which is calculated with the following mixing model:

$$u^s_{k,i,t} = \frac{1}{k_{1k} \cdot c_{s^s_{k,t}} - c_{0^s_{k,t}}} \left[r^s_{k,i,t} \cdot x^s_i \cdot \left(k_{2k} \cdot c_{p^s_{k,i,t}} - c_{sk,t} \right) \right] \tag{A.2}$$

where,

k_{1k}: total reaction rate of pollutants after entering the water body k
k_{2k}: pollution purification rate before entering the water body k
$r^s_{k,i,t} \cdot x^s_i$: discharges into the water body k associated with economic sector i and subregion s, for year t
$c_{p^s_{k,i,t}}$: COD concentration in the discharges to the water body k associated with economic sector i and subregion s
$c_{s^s_{k,t}}$: Standard COD concentration in water body k and subregion s for year t
$c_{0^s_{k,t}}$: COD concentration in water body k and subregion s for year t

Note that $r^s_{k,i,t} = r^s_{k,i} + R^s_{k,i,t}(S^s_t)$ (equation (7) of the article) is completely defined by the hydrological variability in the agricultural sectors. This is the first endogenous component.

The other endogenous component corresponds to $c_{0k,t}$, the COD concentration in the water bodies. We propose an expression for this term that takes into account decreases in COD concentration due to wetter hydrology and increases in COD concentration due to drier hydrology; this is based on the fact that the discharge of organic matter (whose indicator used is COD) depends on the economic system, which, in the case of this work, is considered constant, or more generally, its variability is much smaller than the hydrologic variability.

The variable $\pi^s_{k,t}$ is define by the hydrological model, for groundwater and surface water, like the ratio between the natural supply (hydrological model) in year t and the long-term natural supply, for the water body k and subregion s:

$$\pi^s_{gw,t} \equiv \frac{I^s_t}{I^s} \tag{A.3}$$

$$\pi^s_{sw,t} \equiv \frac{R^s_t}{R^s} \tag{A.4}$$

Let define the following parameters:

$c_{0^{min}_k}$.: Minimum concentration in water body k
$c_{0^{max}_k}$.: Maximum concentration in water body k

$c_{0_k}^{mean}$.: Mean concentration in water body k
π_k^{min}.: Ratio of minimum volume to average volume in water body k
π_k^{max}.: Ratio of maximum volume to average volume in water body k
π_k^{mean}.: Equal to 1 by definition

A linear model is constructed to represent the relationship between the concentration in water bodies before discharge and hydrology (both surface and groundwater). The following linear relation is considered for

$$c_{0_{k,t}} \in \left(c_{0_k}^{min}, c_{0_k}^{max}\right): \quad c_{0_{k,t}}^{s} = a \cdot \pi_{k,t}^{s} + b \tag{A.5}$$

where,

$$a = \frac{c_{0_k}^{max} - c_{0_k}^{min}}{\pi_k^{min} - \pi_k^{max}}$$

$$b = c_{0_k}^{mean}. - a$$

In case of concentrations below the minimum or above the maximum, the ratio of the maximum concentration to the runoff or recharge level indicator (hydrology) is considered constant. Thus, the linear function is defined as follows:

$$c_{0_{k,t}}^{s} = \begin{cases} c_{0_k}^{min} \ \ if\ \pi_{k,t} \le \pi_k^{min}. \\ a \cdot \pi_{k,t} + b \ if\ \pi_k^{min} < \pi_{k,t}^{s} \\ c_{0_k}^{max} \ \ if\ \pi_{k,t} \ge \pi_k^{max} \end{cases} \tag{A.6}$$

When the concentration in the water bodies $\left(c_{0_{k,t}}^{s}\right)$ is higher than the standard concentration in average conditions (c_{sk}), the standard concentration for the year t in subregion s $\left(c_{s_{k,t}}^{s}\right)$ is considered to be that of the water body, since in the model the water for dilution come from the hydrological system. Then:

$$c_{s_{k,t}}^{s} = \begin{cases} c_{s_k}^{s} \ if\ c_{0_{k,t}}^{s} \le c_{sk} \\ c_{0_{k,t}}^{s} \ if\ c_{0_{k,t}}^{s} > c_{sk} \end{cases} \tag{A.7}$$

The additional water for dilution with hydrological variability can be calculated as the difference between the stochastic model coefficient $\left(w_{k,i,t}\right)$ and deterministic model coefficient $\left(w_{k,i}\right)$:

$$H_{k,i,t}^{s}\left[I_t^s, R_t^s, R_{k,i,t}^{s}\left(S_t^s\right)\right] = w_{k,i,t}^{s} - w_{k,i}^{s} \tag{A.8}$$

With this last equation, the input-output model with hydrologic variability is fully determined, including endogenous changes in the water use coefficients, due to the natural hydrologic variability calculated by the multivariate model.

The parameter considered are:

$c_{sk} = 20$ mg/l
$c_{0_k}^{min}. = 15$ mg/l
$c_{0_k}^{max}. = 25$ mg/l
$c_{0_k}^{mean}. = 20$ mg/l
$\pi_k^{min}. = 0.5$
$\pi_k^{max}. = 1.5$
$\pi_k^{mean}. = 1.0$

7.2 Appendix B. Sensitivity analysis of irrigation water losses in Cortona

To assess the implications of assuming a uniform irrigation loss parameter ($\rho = 30\%$) across all agricultural sectors, a univariate sensitivity analysis was conducted. This analysis focuses on the water-stressed region of Cortona, where irrigation losses are expected to have a stronger influence on water scarcity indicators. The parameter ρ was varied within a plausible range between 20% and 40%, and a comparative assessment was performed considering three representative values: 20%, 30%, and 40%. For each value of ρ, total water demand was recalculated, and water scarcity indicators were estimated accordingly. This approach enables the evaluation of the uncertainty range associated with irrigation losses, particularly under extremely dry year conditions.

Table B1 presents the comparison of total water demand across the selected values of ρ, while Table B2 shows the percentage difference relative to the baseline case ($\rho = 30\%$). Figures B1, B2, and B3 present the results of the water scarcity indicators for scenarios with ρ equal to 30%, 20%, and 40%, respectively, whereas Figure B4 and B5 shows the percentage difference of these indicators relative to the baseline case ($\rho = 30\%$).

Table B1
Cortona: Water demand by year and irrigation loss rate

LLS	Irrigation Loss Rate	Demand Category	2014	2015	2016	2017	2018	2019	2020
Cortona	30%	WD	30.2	49.2	30.6	48.3	39.7	32.0	45.1
		ND	19.5	33.2	19.7	32.5	26.4	20.8	30.2
		GD	65.4	65.4	65.4	65.4	65.4	65.4	65.4
		ED	30.9	47.4	29.9	47.1	37.3	33.0	44.1
Cortona	20%	WD	27.9	44.6	28.2	43.7	36.2	29.5	40.9
		ND	17.8	29.8	18.0	29.2	23.8	18.9	27.2
		GD	65.4	65.4	65.4	65.4	65.4	65.4	65.4
		ED	28.9	43.4	27.9	43.1	34.3	30.8	40.4
Cortona	40%	WD	33.3	55.5	33.7	54.3	44.4	35.4	50.6
		ND	21.7	37.7	22.0	36.9	29.7	23.2	34.2
		GD	65.4	65.4	65.4	65.4	65.4	65.4	65.4
		ED	33.5	52.8	32.6	52.4	41.3	36.0	48.9

Source: own elaboration

Table B2
Cortona: Percentage difference of irrigation loss scenarios (ρ = 20% and ρ = 40%) relative to the baseline case (ρ = 30%)

Irrigation Loss Rate	Demand Category	2014	2015	2016	2017	2018	2019	2020	Mean
20%	WD	−8.3%	−10.5%	−8.3%	−10.5%	−9.7%	−8.6%	−10.2%	−9.4%
	ND	−9.4%	−11.4%	−9.4%	−11.3%	−10.6%	−9.7%	−11.1%	−10.4%
	GD	0.0%	0.0%	0.0%	0.0%	0.0%	0.0%	0.0%	0.0%
	ED	−6.8%	−9.4%	−7.1%	−9.3%	−8.7%	−7.3%	−9.0%	−8.2%
40%	WD	9.3%	11.3%	9.3%	11.2%	10.5%	9.6%	11.0%	10.3%
	ND	10.3%	12.0%	10.3%	11.9%	11.3%	10.5%	11.7%	11.2%
	GD	0.0%	0.0%	0.0%	0.0%	0.0%	0.0%	0.0%	0.0%
	ED	7.8%	10.2%	8.2%	10.2%	9.6%	8.3%	9.9%	9.2%

Source: own elaboration

The results show a consistent response of water demand to changes in the irrigation loss rate (ρ) relative to the baseline (30%). Reducing losses to 20% decreases demand by around 8–10%, while increasing losses to 40% raises it by approximately 9–11% across WD, ND, and ED, while GD remains unaffected.

These findings indicate that irrigation losses are a key factor influencing total water demand. Higher loss rates increase the volume of blue water required to meet irrigation needs, reinforcing the substitution of green water by blue water due to inefficiencies in water delivery and application. Conversely, lower losses improve efficiency and reduce blue water withdrawals, therefore, it is important to advance towards estimating this parameter for each local economy.

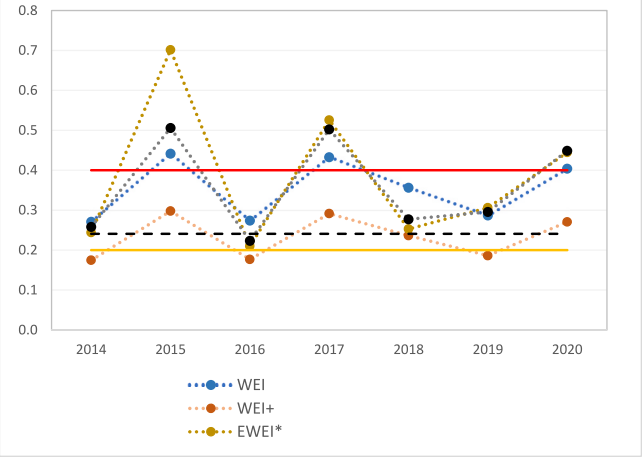

Source: own elaboration

Fig. B1. Blue and grey water scarcity indicators (Cortona, ρ = 30%, baseline case).
Source: own elaboration

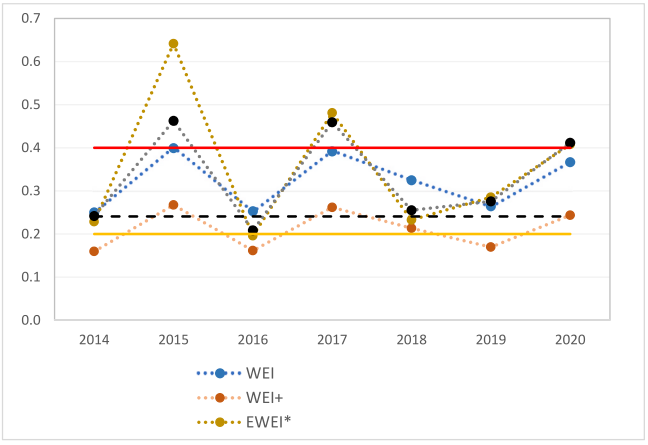

Source: own elaboration

Fig. B2. Blue and grey water scarcity indicators (Cortona, ρ = 20%).
Source: own elaboration

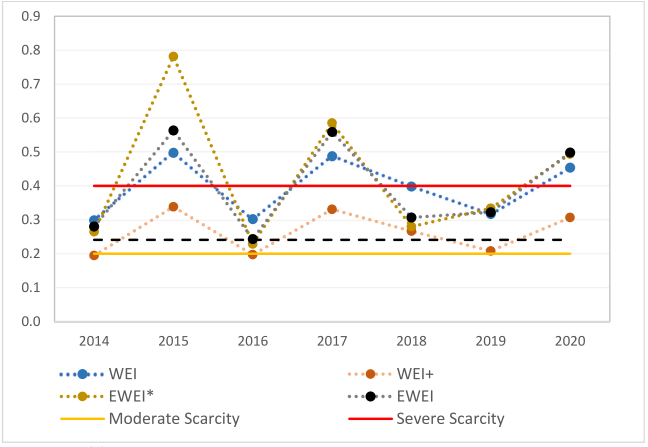

Source: own elaboration

Fig. B3. Blue and grey water scarcity indicators (Cortona, ρ = 40%).
Source: own elaboration

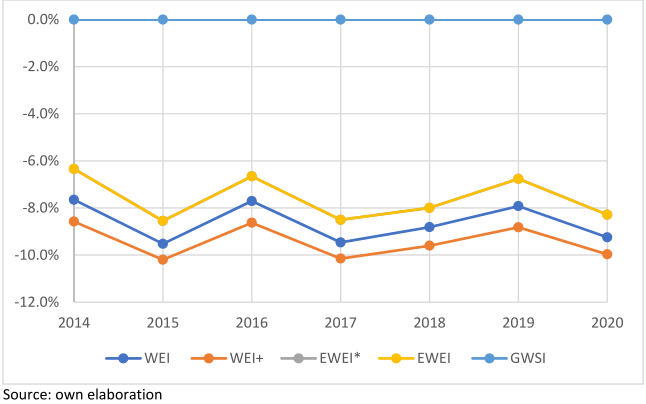

Source: own elaboration

Fig. B4. Difference in water scarcity indicators relative to the ρ = 30% baseline case (Cortona, ρ = 20%).
Source: own elaboration

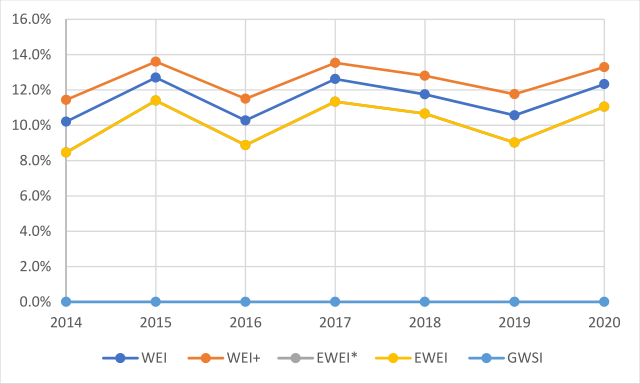

Source: own elaboration

Fig. B5. Difference in water scarcity indicators relative to the ρ = 30% baseline case (Cortona, ρ = 40%).
Source: own elaboration

The results show that water scarcity indicators respond significantly to variations in the irrigation loss rate (ρ). WEI exhibits larger changes compared to WEI+, as it is based on gross water demand, which is directly affected by irrigation losses. In contrast, WEI + shows slightly lower sensitivity since it accounts for net water demand, partially mitigating the effect of losses.

Similarly, EWEI and EWEI* display smaller variations (around 6–11%) compared to WEI and WEI+, as they are based on extended demand (net demand plus grey water), which dilutes the relative impact of irrigation losses. The identical changes observed for EWEI and EWEI* are explained by the fact that only the denominator differs between these indicators, while the demand component responds similarly to changes in ρ.

As expected, Green WE remains unchanged across all scenarios, confirming that it is not affected by irrigation losses.

Overall, the magnitude of the observed changes is significant, particularly under higher loss scenarios, highlighting the strong influence of irrigation efficiency on water scarcity assessments. These findings emphasize the importance of accurately estimating irrigation losses at the local level to improve the robustness and reliability of water scarcity indicators.

Data availability

Data will be made available on request.

References

Alcamo, J., Henrichs, T., Rösch, T., 2000. World Water in 2025: Global Modeling and Scenario Analysis. Kassel World Water Series.

Arnold, J.G., Srinivasan, R., Muttiah, R.S., Williams, J.R., 1998. Large area hydrologic modeling and assessment part I: model development 1. JAWRA Journal of the American Water Resources Association 34 (1), 73–89.

Baggio, G., Qadir, M., Smakhtin, V., 2021. Freshwater availability status across countries for human and ecosystem needs. Sci. Total Environ. 792, 148230.

Bartolini, G., Messeri, A., Grifoni, D., Mannini, D., Orlandi, S., 2014. Recent trends in seasonal and annual precipitation indices in Tuscany (Italy). Theor. Appl. Climatol. 118, 147–157. https://doi.org/10.1007/s00704-013-1053-3.

Bartolini, G., Grifoni, D., Mano, R., Torrigiani, T., Gozzini, B., 2018. Changes in temporal distribution of precipitation in a Mediterranean area (Tuscany, Italy) 1955–2013. Int. J. Climatol. 38, 1366–1374.

Braca, G., Bussettini, M., Lastoria, B., Mariani, S., Piva, F., 2021. *Il Bilancio Idrologico Gis Based a scala Nazionale su Griglia regolare – BIGBANG: Metodologia e stime*. Rapporto sulla disponibilità naturale della risorsa idrica. Istituto Superiore per la Protezione e la Ricerca Ambientale, Roma. Rapporti 339/21.

Braca, G., Bussettini, M., Lastoria, B., Mariani, S., Piva, F., 2022. Il modello di bilancio idrologico nazionale BIGBANG: sviluppo e applicazioni operative. In: *La disponibilità della risorsa idrica naturale in Italia dal 1951 al 2020*. the BIGBANG National Water Balance Model: Development and Operational Applications. *the Availability of Renewable Freshwater Resources in Italy from 1951 to 2020*, 2/2022. L'Acqua.

Chapagain, A.K., Hoekstra, A.Y., 2004. Water Footprints of Nations. UNESCO-IHE. Value of Water Research Report Series No. 16.

Chow, V.T., Maidment, D.R., Mays, L.W., 1988. Applied Hydrology. McGraw-Hill.

Dingman, S.L., 2015. In: Physical Hydrology, 3a ed. Waveland Press.

D'Oria, M., Ferraresi, M., Tanda, M., 2019. Quantifying the impacts of climate change on water resources in northern Tuscany, Italy, using high-resolution regional projections. Hydrol. Process. 33, 978–993. https://doi.org/10.1002/hyp.13378.

El Jeitany, J., Pacetti, T., Caporali, E., 2024a. Evaluating climate change effects on hydrological functionality and water-related ecosystem services. Ecohydrology 17 (4), e2557.

Duarte, R., Serrano, A., Guan, D., Paavola, J., 2016. Virtual Water Flows in the EU27: A Consumption-based Approach. Journal of Industrial Ecology 20 (3), 547–558. https://doi.org/10.1111/jiec.12454.

El Jeitany, J., Nussbaum, M., Pacetti, T., Schröder, B., Caporali, E., 2024b. Landscape metrics as predictors of water-related ecosystem services: insights from hydrological modeling and data-based approaches applied on the Arno river basin, Italy. Sci. Total Environ. 954, 176567.

European Environment Agency, 2020. Use of freshwater resources in Europe. https://www.eea.europa.eu/data-andmaps/indicators/use-of-freshwater-resources-3/assessment-4.

Faergemann, H., 2012. "Update on water scarcity and droughts indicator development. In: EC Expert Group on Water Scarcity & Droughts. European Environment Agency, Brussels, Belgium, pp. 1–23.

Fatichi, S., Caporali, E., 2009. A comprehensive analysis of changes in precipitation regime in Tuscany. Int. J. Climatol. 29, 1883–1893. https://doi.org/10.1002/joc.1921.

Feng, K., Hubacek, K., Pfister, S., Yu, Y., Sun, L., 2014. Virtual scarce water in China. Environ. Sci. Technol. 48 (14), 7704–7713. https://doi.org/10.1021/es500502q.

Guan, D., Hubacek, K., 2008. A new and integrated hydro-economic accounting and analytical framework for water resources: a case study of North China. J. Environ. Manag. 88, 1300–1313.

Hoekstra, A.Y., 2016. A critique on the water-scarcity weighted water footprint. Ecol. Indic. 66, 564–573. https://doi.org/10.1016/j.ecolind.2016.02.026.

IPCC, 2021. In: Masson-Delmotte, V., Zhai, P., Pirani, A., Connors, S.L., Péan, C., Berger, S., Zhou, B. (Eds.), Climate Change 2021: the Physical Science Basis. Contribution of Working Group I to the Sixth Assessment Report of the Intergovernmental Panel on Climate Change. Cambridge University Press. https://doi.org/10.1017/9781009157896.

IRPET, 2021. Interregional Input-Output Table for the Tuscany Region, Italy. Istituto Regionale di Programmazione Económica Regione Toscana.

ISTAT, 2019. Water Use and Quality in Italy. Istituto Nazionale di Statistica, Italia. https://www.istat.it/it/archivio/234904.

ISTAT, 2021. Banchi di dati e sistemi informazioni. https://www.istat.it/it/dati-analisi-e-prodotti/banche-dati.

Miller, T., Blair, P., 2022. Input-Output Analysis: Foundations and Extensions, 3nd Edition. Cambridge University Press.

Northern Apennine District Authority, 2021. *Piano di Gestione delle Acque del Distretto Idrografico dell'Appennino Settentrionale*. Aggiornamento ciclo 2021-2027. Firenze, Dicembre 2021.

OECD, 2015. Water: Freshwater Abstractions (Edition 2015). OECD Environment Statistics. https://doi.org/10.1787/f9f5fcd1-en (database).

Pacetti, T., Castelli, G., Schröder, B., Bresci, E., Caporali, E., 2021. Water ecosystem services footprint in agricultural production in central Italy. Sci. Total Environ. 797, 149095.

Pacetti, T., Sturla, G., El Jeitany, J., Rocchi, B., Biscarini, C., Caporali, E.C., 2026. Linking water footprint and social vulnerability: a sub-regional input–output framework for assessing multiple dimensions of water scarcity. Front. Water 8, 1802261. https://doi.org/10.3389/frwa.2026.1802261.

Pfister, S., Koehler, A., Hellweg, S., 2009. Assessing the environmental impacts of freshwater consumption in LCA. Environ. Sci. Technol. 43 (11), 4098–4104. https://doi.org/10.1021/es802423e.

Pranzine, G., Di Martino, F., Della Santa, E., Fontanelli, K., Fucci, G., 2020. Impact of climate change on the water balance of the Apuo-Versilia plain aquifer (Tuscany, Italy). Italian Journal of Groundwater. https://doi.org/10.7343/as-2020-474.

Ridoutt, B.G., Hadjikakou, M., Nolan, M., Bryan, B.A., 2018. From water-use to water-scarcity footprinting in environmentally extended input–output analysis. Environ. Sci. Technol. 52, 6761–6770.
Rijsberman, F.R., 2006. Water scarcity: fact or fiction? Agric. Water Manag. 80 (1–3), 5–22.
Rocchi, B., Sturla, G., Viccaro, M., 2024. A hydro-economic input-output model to assess economic pressures on water resources. Bio base Appl. Econ. 13 (2), 203–2017.
Rocchi, B., Paniccià, R., Sturla, G., 2026. Hydro-economic equilibrium with climatic variability in interconnected local economies. Ecol. Econ. 239, 108790. https://doi.org/10.1016/j.ecolecon.2025.108790.
Rossi, G., Benedini, M. (Eds.), 2020. *Water Resources of Italy: Protection, Use and Control* (World Water Resources, vol. 5. Springer.
Rossi, G., Caporali, E., 2010. Regional analysis of low flow in Tuscany (Italy). In: Global Change: Facing Risk and Threats to Water Resources, vol. 340. IAHS Publ.
SIR Toscana, 2021. Strati GIS. https://www.sir.toscana.it/strati-gis.
Sturla, G., Rocchi, B., 2024. Effects of hydrological variability on the sustainable use of water in a regional economy. An application to Tuscany. Environ. Sustain. Indic. 24, 100448.
Sturla, G., Ciulla, L., Rocchi, B., 2023. Natural and social scarcity in water footprint: an input-output analysis for Italy. Ecol. Indic. 147, 1–20.
UN WWDR, 2024. The United Nations World Water Development Report 2024: Water for Prosperity and Peace. UNESCO, Paris, 2024.
Venturi, C., Campo, L., Caparrini, F., Castelli, F., 2014. The assessment of the water consumption at regional scale: an application in Tuscany, Central Italy. European Water 46/46, 3–23.
Wang, D., Hubacek, K., Shan, Y., Gerbens-Leenes, W., Liu, J., 2021. A review of water stress and water footprint accounting. Water 13 (2), 201. https://doi.org/10.3390/w13020201.
Wichelns, D., 2017. Volumetric water footprints, applied in a global context, do not provide insight regarding water scarcity or water quality degradation. Ecol. Indic. 74, 420–426.
Xie, Y., 1996. "Environment and Water Quality Model". China Science and Technology Press, Beijing, China.
Zhao, S., Lin, J., Cui, S., 2011. Water resource assessment based on the water footprint for Lijiang city. Int. J. Sustain. Dev. World Ecol. 18 (6), 492–497.